13th International Symposium on Turbulence and Shear Flow Phenomena (TSFP13)
Montreal, Canada, June 25–28, 2024

SELF-SIMILARITY FOR TURBULENCE STATISTICS OF LOGARITHMIC REGION IN HIGH REYNOLDS NUMBER PIPE FLOW

Noriyuki Furuichi
National Metrology Institute of Japan
Advanced Industrial Science and Technology
1497-1 Teragu Tsukuba
furuichi.noriyuki@aist.go.jp

Marie Ono
National Metrology Institute of Japan
Advanced Industrial Science and Technology
1497-1 Teragu Tsukuba
ono.marie@aist.go.jp

Yoshiyuki Tsuji
Graduate school of engineering
Nagoya University
Furo-cho, Nagoya, Aichi
c42406a@cc.nagoya-u.ac.jp

ABSTRACT

A self-similarity of turbulence statistics for 3 velocity components in high Reynolds number pipe flow is discussed based on detailed experimental results from $Re_\tau = 11200$ to 20750 using LDV at Hi-Reff. Two logarithmic slopes in the turbulence intensity profiles are observed in the logarithmic region of the mean velocity profile. Self-similarity is observed at $Re_\tau = 20750$ in the higher order moments and KLD profiles at the near-wall side in the logarithmic region of the mean velocity profile. However, in the outer logarithmic region, self-similarity is not observed. It is suggested that the characteristics of the turbulence statistics in the inner side in the logarithmic region are more consistent with the attached eddy hypothesis than in the outer side.

INTRODUCTION

One of the important research subjects for wall-bounded flows is the establishment of scaling laws for mean velocity and turbulence intensity profiles. Among the scaling laws focused on in the previous studies, the logarithmic behaviour would be the most fundamental but important one in the wall-bounded flow. The well-known logarithmic behaviour is observed in not only in the mean velocity profile but also in the turbulence intensity profile. The turbulence intensity around y/R=0.1 is given by the following:

$$\langle (u'^{+})^2 \rangle = B_{1,u} - A_{1,u} \ln(y/R) \qquad (1)$$

where R is the outer length scale (radius of the pipe) and u' is the streamwise velocity fluctuation. $A_{1,u}$ and $B_{1,u}$ are constants. In this paper, the bracket $\langle\rangle$ denotes the mean value. Marusic et al. (2013) mentioned that both logarithmic regions in the mean velocity and Eq. (1) are almost consistent. If this is true, the cross-plot between the mean velocity and turbulence intensity profiles would show a linear relationship. However, as shown in Fig. 1 based on our previous result (Ono et al., 2022), the linear relation does not cover all logarithmic region in mean velocity profile, rather two linear relations are

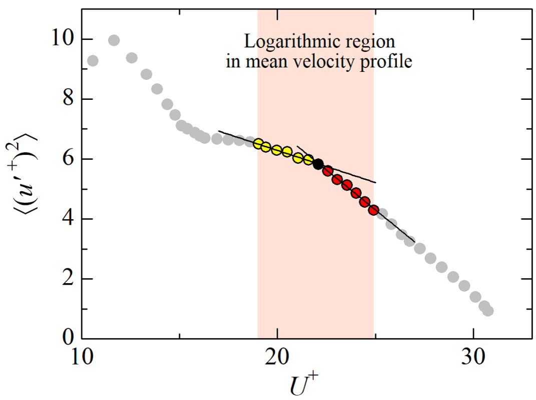

Figure 1. Cross plot between mean velocity and turbulence intensity profiles at $Re_\tau = 20750$ in pipe flow.

observed in this result. To clarify the reason for this inconsistency is the main subject of the present paper.

The existence of the logarithmic layer in the turbulence intensity was suggested by the attached eddy hypothesis (Townsend 1976, hereinafter AEH) and was modelled by Perry and Chong (1982) that the population density of eddies attached to the wall varies inversely with the distance from the wall. In the last decade, studies at high Reynolds numbers (e.g. Hultmark et al. 2013) have provided clear evidence for the existence of a logarithmic region in the turbulence intensity profiles and strongly support the AEH from the perspective of turbulence statistics. The AEH gives the following relationships for the wall-normal and spanwise velocity components:

$$\langle (v'^{+})^2 \rangle = B_{1,v} \qquad (2)$$

$$\langle (w'^{+})^2 \rangle = B_{1,w} - A_{1,w} \ln(y/R) \qquad (3)$$

where v' and w' are the wall-normal and spanwise velocity

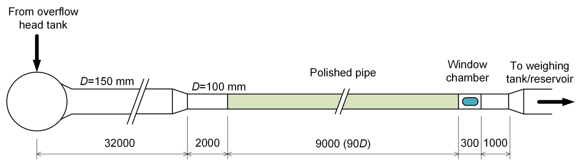

Figure 2. Schematic of experimental pipe layout. The glass pipe is installed in the window chamber.

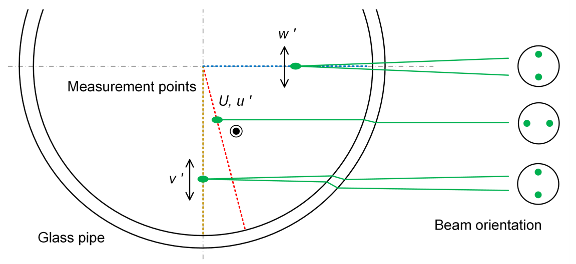

Figure 3. The measurement line for 3 velocity components and beam alignment of LDV system.

fluctuations, respectively. The AEH includes the critical assumptions that characteristic attached eddies are self-similar, i.e. their energy density is constant and their overall geometry scales only with distance from the wall. With these and other assumptions, Townsend (1976) derived the turbulent intensity distributions with the distance from the wall, which are Eqs. (1)-(3). For this strict assumption, Baars et al. (2017) defined structures that are attached to the wall and showed that these structures are self-similar with a constant streamwise/wall-normal aspect ratio by two-point measurements in the wall-normal direction and spectral coherence analysis. However, the self-similarity in perspective of the turbulence statistics is difficult to find in the logarithmic region of the turbulence intensity profile and the discussion is still ongoing. For example, Perry et al. (1986) predicted that the self-similar structure according to the AEH leads the spectral slope of k^{-1}. However, experimental and numerical studies have so far shown no clear evidence for the k^{-1} spectrum thus far, although the logarithmic region of Eq. (1) has been observed (e.g. Vallikivi et al. 2015). Baars et al., (2020) proposed the superimposed turbulence intensity profile and mentioned that the Reynolds number in the existing experimental result is too low to observe the k^{-1} spectrum. Furthermore, the Hwang et al., (2022) mentioned that the k^{-1} spectrum is not necessary condition to establish the logarithmic behaviour in the turbulence intensity profile.

In this paper, we discuss the self-similarity in perspective of the probability density function (PDF) for three velocity components in high Reynolds number pipe flow. If the attached eddies have a self-similar distribution in space, the velocity fluctuations caused by them are expected to be invariant independently of the wall-normal position in the logarithmic region. We discuss the similarities by higher order moment and Kullback-Leibuler divergence (KLD) analysis in this paper to consider about the strict establish region of Eqs. (1)-(3) according to AEH based on reliable experimental data for the three components measured in this study.

EXPERIMENTS

Experiments were conducted in high Reynolds number actual facility (Hi-Reff). The working fluid in this facility is water. Hi-Reff equips the overflow head tank suppling stable flow to the test section, the large capacity underground storage tank to achieve high stability of water temperature and the static gravimetric weighing tank to measure high accurate flowrate. The schematic of the testing line is shown in Fig. 2. The straight pipe with $D = 100$ mm has length of $110D$ and the $90D$ within it is carefully polished with mean roughness Ra is $0.1\mu m$. At the downstream of the polished pipe, the window chamber with a glass pipe was installed. The glass pipe is also well polished to achieve a high roundness of the inner diameter and a small tolerance of the glass wall thickness.

The velocity measurement was conducted by laser Doppler velocimetry (LDV). By changing the beam orientation and the measurement line as shown in Fig. 3, 3 velocity components were measured. The control lengths that affect to the measurement result are $L_{\mathrm{v}}^{+} = 29$ for v component and $L_{\mathrm{w}}^{+} = 190$ for w at $Re_\tau = 20750$. L_{u}^{+} for u component depends on the wall-normal position and is e.g. $L_{\mathrm{u}}^{+} = 18$ at $y^{+} = 15$ and $L_{\mathrm{u}}^{+} = 59$ at $y^{+} = 400$. The correction for the spatial resolution was conducted according to the analysis by Durst et al., (1995). In addition, the correction for the passing frequency of particles and the fringe distortion were also conducted. The details of the correction procedure are shown in our previous paper (Ono et al., 2022).

The range of Reynolds numbers examined in this experiment was from $Re_\tau = 990$ to 20750. The detailed experimental results for the 3 component turbulence intensity profiles have been reported in Ono et al., (2023). In this paper, we mainly focus on the experimental result at $Re_\tau = 11200$ and 20750. The bulk velocity is calculated from the flowrate, which is measured using gravimetric weighing tank. The wall shear stress for the friction velocity is calculated from the friction coefficient given by Furuichi et al., (2015).

RESULTS AND DISCUSSION

Mean velocity and turbulence intensity profiles for 3-components

The mean velocity profile and the 3-component turbulence intensity profiles at $Re_\tau = 11200$ and 20750 are shown in Fig. 4. The details of the symbols and lines are described in the caption of this figure. Based on the difference of the linear relation shown in Fig. 1, the logarithmic region for near-wall side is referred to as the " inner-log region " and outer side is as the " outer-log region ". The logarithmic region of the streamwise component in previous high Reynolds number research would correspond to the outer-log region (e.g. Marusic et al., 2013). In fact, the logarithmic slope can be observed in the streamwise and spanwise component in the outer-log region and those slopes are almost consistent with the previous works (see Ono et al., 2023). Here, we focus on the region where Eqs. (1)-(3) according to the assumption of AEH satisfy. Eqs. (1)-(3) should be established in the same region. As mentioned above, the logarithmic region in the streamwise and the spanwise turbulence intensity profiles are investigated in the same region, which is the outer-log region. For the wall-normal component, according to Eq. (3), the constant region should be observed in the same region. However, the turbulence intensity profile of the wall-normal component does not show the constant value in the outer-log region.

Next, we investigate the inner-log region. As shown by the lines in Fig. 4, the logarithmic slopes are also observed in

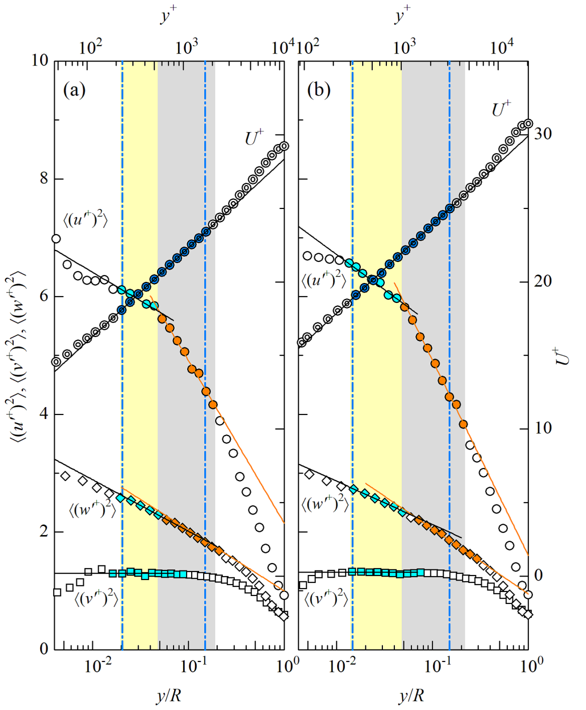

Figure 4. Mean velocity and turbulence intensity profiles at (a) $Re_\tau = 11200$ and (b) $Re_\tau = 20750$. Solid black and orange lines are obtained by the fitting to experimental result to Eqs. (1)-(3). Light blue and orange symbols are the experimental result used to the fitting. The blue long and short alternative dashed lines are the start and end points of the logarithmic region of mean velocity profiles. The logarithmic region of the mean velocity profile is divided two regions with yellow and gray shaded based on the lines according to Eq. (1)-(3). The yellow shaded region is referred as the inner-log region and gray is the outer-log region.

the streamwise and spanwise components. Furthermore, the constant region in the wall-normal component is clearly observed in the inner-log region. From the turbulence intensity profiles obtained in this experiment, it is suggested that only the inner-log region satisfies all of Eqs. (1)-(3). Since this region is inconsistent with the previous studies (e.g. Marusic et al., 2013), the difference of the turbulence statistics between the two logarithmic regions is discussed in the next section.

The coefficients of each fitting line in both log region according to Eqs. (1)-(3) have Reynolds number dependence, although they have a large uncertainty due to fewer data points to calculate them. In the previous papers, the coefficients are expected to be universal. However, the recent study by Hwang et al. (2022) mentioned that they have a Reynolds number dependence. Even the logarithmic slope in the mean velocity profile is still under discussion and this indicates the difficulty in obtaining the logarithmic slope precisely. Further works are necessary to determine the logarithmic slope of the turbulence intensity profile.

Several relations between the logarithmic region in mean velocity and turbulence intensity profiles are mentioned in this paper. It is clearly found that the logarithmic region in the mean velocity profile is covered by the inner-log and outer-log region of the turbulence intensity profile. The starting points according to Eqs. (1)-(3) and the logarithmic region of the mean velocity profile are well consistent each component. The

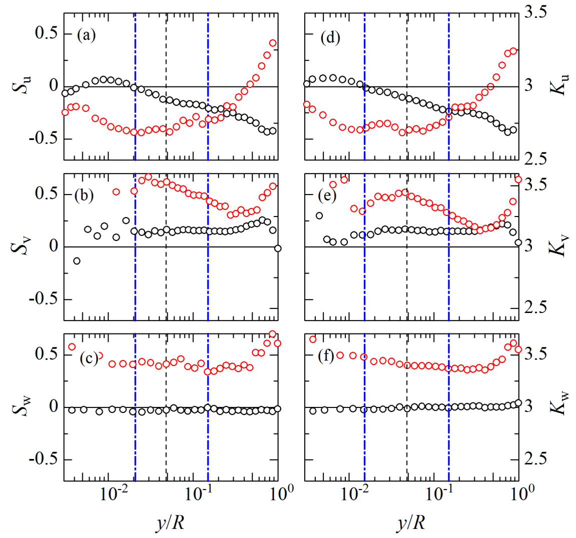

Figure 5. Skewness (S) and kurtosis (K) for three velocity components at (a)(b)(c) $Re_\tau = 11200$, (d)(e)(f) $Re_\tau = 20750$. White circles are skewness and red are kurtosis. The blue long and short alternative dashed lines are the start and end points of the logarithmic region of mean velocity profiles. The black dashed line is the bound between the inner-log and outer-log regions.

end point of the inner-log region (or the start point of the outer-log region) are similar for the streamwise and spanwise component. Only the wall-normal component, the region according to Eq. (2) is larger than other components. On the other hand, the end point of the outer-log region is not consistent each component including the mean velocity profile.

Higher order moment

As mentioned, the assuming in the AEH means a self-similar structure in the logarithmic region. As the logarithmic law in the mean velocity distribution implies the existence of a constant stress layer, the emergence of logarithmic behaviour in the turbulence intensity profile also implies self-similarity in the turbulence statistics. In this paper, the self-similarity of the turbulence statistics according to the AEH is considered from the probability density function (PDF). To investigate the PDF form, the profiles of the skewness and kurtosis are shown in Fig. 5 as firstly. If the PDF form normalized by the standard deviation has self-similarity, both skewness and kurtosis profiles are expected to be constant. Therefore, they are constant at the regions where Eqs. (1)-(3) are established according to the AEH. However, no region satisfies it completely in Fig. 5 although only the spanwise component has almost similar normalized PDF in the logarithmic region.

On the other hand, the kurtosis profiles show important feature regarding the inner-log and outer-log region. The kurtosis in the streamwise and wall-normal components shows clear difference between the inner-log and outer-log regions and seems to be nearly constant in the inner-log region. Here, we make attention to the even order moment in the following. Several studies have reported that the logarithmic behaviour in the turbulence intensity distribution is also observed in the profile of even order higher moments (e.g. Meneveau and Marusic, 2013). The profiles of even order higher moment at $Re_\tau = 20750$ for each compoenent are shown in Fig. 6. Although the scattering of the data is investigated in the higher

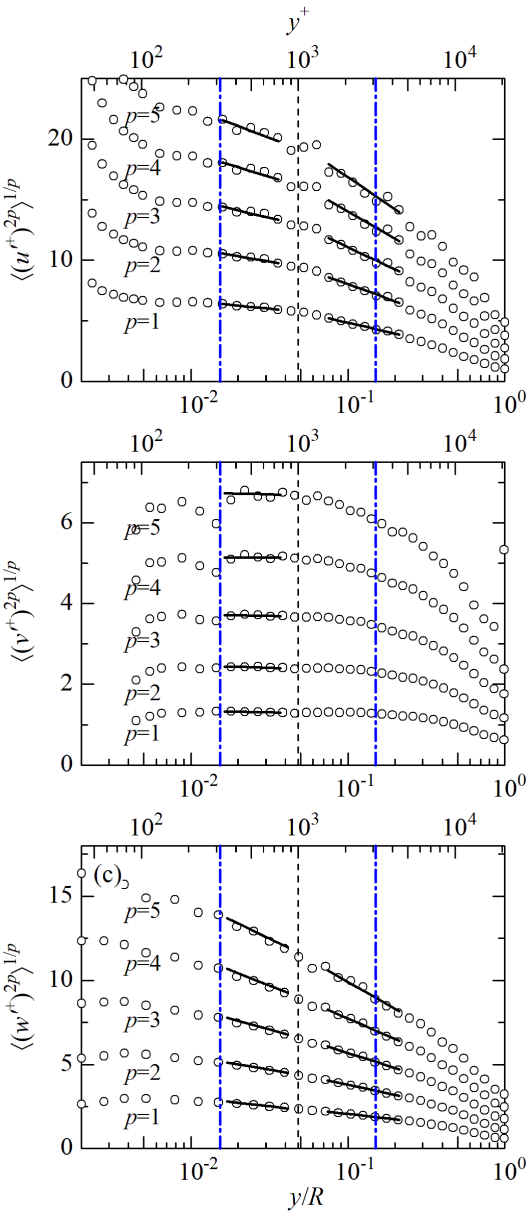

Figure 6. Higher order moments for three velocity components at $Re_\tau = 20750$. The blue long and short alternative dashed lines are the start and end points of the logarithmic region of mean velocity profiles.

order moment, the profiles for the streamwise and spanwise component have logarithmic relations up to $p = 5$ in both log regions. The most significant point of this result is suggesting the existence of the self-similarity in the wall-normal component. The higher order moment in the wall-normal component indicates constant value in the inner-log region but not in the outer-log region. The skewness is also constant in the logarithmic region. Therefore, it is concluded that the normalized PDF for the wall-normal component is invariant in the inner-log region. Thus, the difference between the inner and outer log-region in the wall-normal component is more clearly observed in the higher order moment.

We conduct further consideration for the streamwise component. The equation of the logarithmic region in higher order moment for streamwise component is given by the following,

$$\langle u'^{+2p} \rangle^{1/p} = B_{p,u} - A_{p,u} \ln(y/R). \tag{4}$$

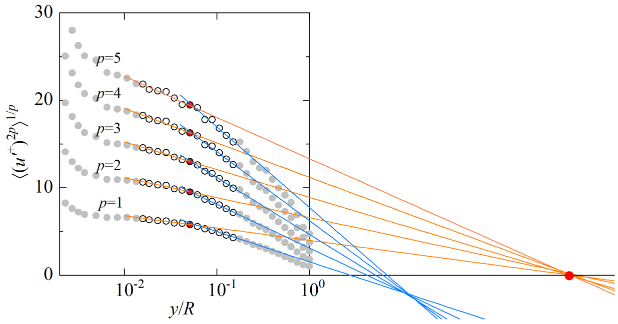

Figure 7. x-intercept of Eq. (6) for streamwise component at $Re_\tau = 20750$. Orange lines are the fitting line for the inner-log region and blue are for outer-log region.

Here, the higher-order moments normalized by the 2nd-order moment are defined as follows:

$$\langle u'^{+2p} \rangle / \langle u'^{+2} \rangle^p = M_{2p}. \tag{5}$$

Substituting Eqs. (1) and (4) into Eq. (5), then,

$$B_{1,u} - A_{1,u} \ln(y/R) = M_{2p}^{1/p} \{ B_{p,u} - A_{p,u} \ln(y/R) \}. \tag{6}$$

When the logarithmic relation in the right and left-hand side term is established in the same y/R location, the normalized even moments $M_{2p}^{1/p}$ must take the constant value at any y location in the logarithmic region. Therefore, the logarithmic region in even order higher moment indicates the existence of the invariant region of the moment. Using the y/R position where $\langle u'^{+2p} \rangle^{1/p} = 0$ in Eq. (4), namely x-intercept, the evidence for invariant of the moment is shown in this report. When Eq. (6) is established, therefore $M_{2p}^{1/p}$ is constant, the x-intercept must be same for each order of the moment. The expansion of the fitting curves for streamwise component is shown in Fig. 7. The fitting curve for the inner-log region has clearly same x-intercept for each order of the moment. This result indicates that the inner-log region satisfies the invariance of the even moment. On the other hand, the fitting curve for the outer-log region does not have same x-intercept although they are crossed at one point. Therefore, the outer-log region does not satisfy the invariance of the even moment. Since the skewness has the dependence of the wall-normal position in both log regions, the self-similar of the turbulence statistics for 3 velocity component is not observed. However, it is possible to say that the characteristics of the turbulence statistics in the inner-log region is more consistent with the assuming of AEH than the outer-log region.

Divergence

To evaluate the invariant region of a PDF in further, the Kullback-Leibuler divergence (KLD) as following is useful (Tsuji et al., 2005),

$$D(P||Q) \equiv \sum_{s_i} p(s_i) \log \frac{p(s_i)}{q(s_i)}. \tag{7}$$

where $p(s_i)$ and $q(s_i)$ are the discrete PDFs. This formula gives a quantitative value regarding the similarity between

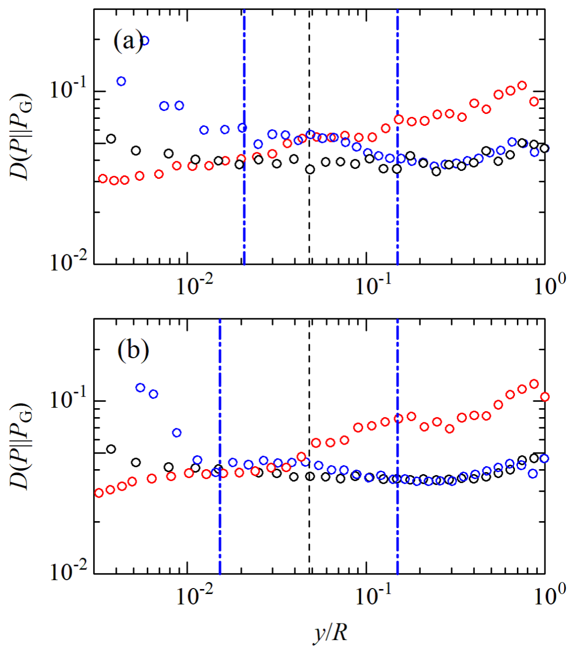

Figure 8. Profiles of KLD at (a) $Re_\tau = 11200$, (b) $Re_\tau = 20750$. Red circles are the streamwise component, Blue are the wall-normal, Black are the spanwise.

two PDFs. The KLD profiles for each velocity component are shown in Fig. 8, where $p(s_i)$ adopts a Gaussian profile. The PDF invariant region for all components is not observed at $Re_\tau = 11200$, but it emerges in the inner-log region at $Re_\tau = 20750$. As Barrs et al,(2022) mentioned, the experiments in sufficient high Reynolds number is necessary to observe the self-similarity according to AEH. Although it is still unclear that $Re_\tau = 20750$ is sufficient to observe it, the result of KLD profile shown in Fig. 8 is one of the evidence which the PDF have self-similarity in the inner-log region. On the other hand, the KLD in the outer-log region does not show the invariant behaviour. KLD of the streamwise component increases toward the outside of the outer logarithmic region, while the wall-normal and spanwise components show nearly invariant profiles. From those results, it is suggested that the PDFs in the inner-log region show self-similar, but the outer-log region do not. This is not direct evidence to satisfy the assumptions of AEH. However, this result also indicates that the characteristics of the turbulence statistics in the inner-log region is more consistent with the assumption of AEH than the outer-log region.

CONCLUSION

The self-similarity of the turbulence statistics for 3 velocity components in high Reynolds number pipe flow was discussed based on the detail experimental results using LDV at Hi-Reff. The self-similarity was observed at $Re_\tau = 20750$ in the higher order moments and KLD profiles at the near-wall side of the logarithmic region in the mean velocity profile, namely the inner-log region. However, at the far-wall side, namely the outer-log region, it was not observed. The characteristics of the turbulence statistics in the inner-log region is suggested to be more consistent with the assuming of the AEH than the outer-log region.

REFERENCES

Baars, W. J., Hutchins, N. and Marusic, I., 2017, "Self-similarity of wall-attached turbulence in boundary layers", J. Fluid Mech., 823, R2.

Baars, W. J. and Marusic, I., 2020, "Data-driven decomposition of the streamwise turbulence kinetic energy in boundary layers", Part 2. Integrated energy and A1. J. Fluid Mech., 882, A26.

Durst, F., Jovanović, J. and Sender, J., 1995, "LDA measurements in the near-wall region of a turbulent pipe flow", J. Fluid Mech., 295, 305–335.

Furuichi, N., Terao, Y., Wada, Y. and Tsuji, Y., 2015, "Friction factor and mean velocity profile for pipe flow at high Reynolds numbers", Phys. Fluids, 27(9).

Hultmark, M., Vallikivi, M., Bailey, S. C. C. and Smits, A. J., 2013, "Logarithmic scaling of turbulence in smooth- and rough-wall pipe flow", J. Fluid Mech., 728, 376-395.

Hwang, Y., Hutchins, N. and Marusic, I., 2022, "The logarithmic variance of streamwise velocity and conundrum in wall turbulence", J. Fluid Mech., 933, A8.

Marusic, I., Monty, J. P., Hultmark, M. and Smits, A. J., 2013, "On the logarithmic region in wall turbulence", J. Fluid Mech., 716, R3.

Meneveau, C. and Marusic, I., 2013, "Generalized logarithmic law for high-order moments in turbulent boundary layers", J. Fluid Mech., 719(December 2012), 1–11.

Ono, M., Furuichi, N., Kurihara N., Wada Y. and Tsuji, Y., 2022, "Reynolds number dependence of inner peak turbulence intensity in pipe flow", Phys. Fluids, 34, 045103.

Ono, M., Furuichi, N. and Tsuji, Y., 2023, "Reynolds number dependence of turbulent kinetic energy and energy balance of the 3-component turbulence intensity in a pipe flow", J. Fluid Mech., 975, A9.

Perry, A. E. and Chong, M. S., 1982, "On the mechanism of wall turbulence", J. Fluid Mech., 119, 173–217.

Perry, A. E., Henbest, S. and Chong, M. S., 1986, "A theoretical and experimental study of wall turbulence", J. Fluid Mech.,165, 163–199.

Townsend A.A., 1976, "The structure of turbulent shear flow", vol 2, Cambridge University Press.

Tsuji, Y., Lindgren, B. and Johansson, A. V., 2005, "Self-similar profile of probability density functions in zero-pressure gradient turbulent boundary layers", Fluid Dynamics Research, 37(5), 293–316.

Vallikivi, M., Hultmark, M. and Smits, A. J., 2015, "Turbulent boundary layer statistics at very high Reynolds number", J. Fluid Mech., 779, 371–389.